Multi-Type Map Construction via Semantics-Aware Autonomous Exploration in Unknown Indoor Environments

Jianfang Mao†, Yuheng Xie†, Si Chen†, Zhixiong Nan*,
Xiao Wang, *Senior Member*, *IEEE*

Abstract— **This paper proposes a novel semantics-aware autonomous exploration model to handle the long-standing issue: the mainstream RRT (Rapid-exploration Random Tree) based exploration models usually make the mobile robot switch frequently between different regions, leading to the excessively-repeated explorations for the same region. Our proposed semantics-aware model encourages a mobile robot to fully explore the current region before moving to the next region, which is able to avoid excessively-repeated explorations and make the exploration faster. The core idea of semantics-aware autonomous exploration model is optimizing the sampling point selection mechanism and frontier point evaluation function by considering the semantic information of regions. In addition, compared with existing autonomous exploration methods that usually construct the single-type or 2-3 types of maps, our model allows to construct four kinds of maps including point cloud map, occupancy grid map, topological map, and semantic map. To test the performance of our model, we conducted experiments in three simulated environments. The experiment results demonstrate that compared to Improved RRT, our model achieved 33.0% exploration time reduction and 39.3% exploration trajectory length reduction when maintaining >98% exploration rate.**

I. Introduction

Map construction via autonomous exploration is a task that a robot moves in an unknown environment and synchronously construct the map of the environment, which is significant for robotic systems. The widely-used exploration strategy adopts the frontier-based mechanism [1], [2], [3]. In the seminal work of the frontier-based methods [1], a robot firstly detects the frontier between the unknown region (the region that has not been explored) and the known region (i.e., the region that has been explored) using the laser scanner. Then, some candidate frontier points are generated based on the frontier. Subsequently, the nearest frontier point is selected robot's moving goal. The above steps are repeated to finally realize the exploration of the whole environment. Based on the frontier-based mechanism, the NBV (Next-Best-View) based exploration mechanism optimizes the candidate frontier points evaluation function to determine the robot's next viewpoint goal, by considering the information gain [4], path cost [5], and other factors [6] of frontier points. Apart from the above exploration mechanics, some methods [7], [8], [9], [10], [11] propose the sample-based mechanism to perform the exploration.

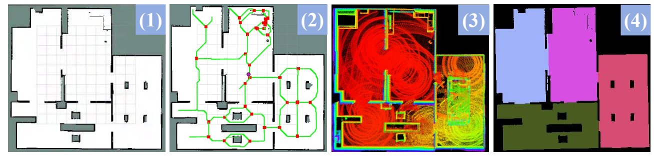

Fig. 1: Four kinds of maps constructed by our semantics-aware autonomous exploration model. (1) 2D occupancy grid map, (2) topological map, (3) 3D point cloud map, and (4) semantic map.

These methods have largely pushed forward the research of autonomous exploration, but present two insufficiencies. *1) Existing autonomous exploration methods do not simultaneously generate the rich types of maps*. Some works only generate single-type map like 2D occupancy grid maps [1], [11] or 3D point cloud maps [12]. Some works attempt to construct multi-type maps via autonomous exploration. For example, the methods of [13], [14], [15] generate 2D occupancy grid map and topological map; The work [16] generates 3D point cloud map, topological map and semantic information. However, the types of maps are still incomplete. The potential reason is that generating more types of maps needs to consider many factors such as the coordinate consistency and the computation conflict.

2) Existing autonomous exploration methods usually execute the excessively-repeated explorations for the same region. When reproducting existing methods, we find it is a common case that a robot moves to the next region when the current region has not been fully explored, which easily generates repeated exploration trajectories and significantly affects the exploration efficiency. We analyze the two-fold reasons with RRT-based exploration. First, due to the randomness of sample point generation, it is difficult to stably guarantee that the best next viewpoint is always inside the current region before it is fully explored. Second, the frontier point evaluation function does not consider the semantic region information of environment when determining the next best viewpoint, so it is easy to select the frontier point (closer to other bigger unknown space) as the best viewpoint.

To handle the above two insufficiencies, this paper proposes a semantics-aware autonomous exploration model, which encourages a mobile robot to fully explore the current

Jianfang Mao, and Zhixiong Nan are with the Chongqing University, Chongqing 400044, China.

Yuheng Xie is with the Chongqing University of Posts and Telecommunications, Chongqing 400065, China.

Si Chen is with the Information Science Academy, China Electronics Technology Group Corporation, Beijing 100086, China.

Xiao Wang is with the School of Artificial Intelligence, Anhui University, Hefei 230031, China, and also with the State Key Laboratory for Management and Control of Complex Systems, Institute of Automation, Chinese Academy of Sciences, Beijing 100190, China.

† Jianfang Mao, Yuheng Xie, and Si Chen are co-first authors.

∗ Zhixiong Nan is the corresponding author.

region before moving to the next region. The proposed model is able to achieve faster speed by avoiding a robot to come back again to the current region to explore the previously-unexplored space, which is implemented by proposing a new frontier point generation mechanism and a new evaluation function that take the semantic region information of environments into consideration. In addition, the proposed autonomous exploration model could generate four types of maps (including 2D occupancy grid map, 3D point cloud map, topological map, and semantic map, as shown in Fig. 1) while maintaining the real-time exploration at the same time.

In the experiments, our model is compared with original RRT [10], TOPO [15], Improved RRT and MMPF (proposed in [17]) in three simulated environments. Compared to Improved RRT, our model achieved **33.0%** exploration time reduction and **39.3%** exploration trajectory length reduction when maintaining $>$**98%** exploration rate. We also compared the map types with the existing methods and analyzed the storage sizes and update time of different kinds of maps.

The contributions of this paper are as follows:

- this paper proposes a semantics-aware autonomous exploration model, which is able to avoid excessively-repeated explorations for the same region.
- the proposed autonomous exploration model allows to simultaneously construct four kinds of maps in unknown indoor environments.

II. Related Work

A. Autonomous Exploration Strategy

The widely-used exploration strategy for robots include the frontier-based mechanism [1], [2], [3] and the NBV-based mechanism [4], [5], [6]. The frontier-based mechanism guides the robot greedily towards unknown areas that may provide new information [1], while in NBV-based exploration, candidate frontier points are considered in more detail for determining the next viewpoint goal. In the work [4], the evaluation of frontier points takes into account the information gain while reducing the uncertainty in the robot's closed-loop actions. In addition to incorporating information gain, path cost is also considered in NBV evaluation [5].

The sample-based exploration mechanism, with the typical representative being the RRT family [7], [8], [9], [10], [11] is suitable for navigation in complex or large-scale environments. In the work [7], to improve the sampling efficiency of the original RRT, the idea of a disjointed tree was proposed. RRT continuously selects random points on the map as the target points for the growth of each branch, and frontier points are generated when the branch reaches the frontier [10].

Although the RRT-based exploration has a high exploration rate in the exploration of complex environments, it can lead to the problem of excessive repetition in exploration due to the randomness of sample point selection. By combining the semantic map, we also consider the semantic region information in addition to information gain and path cost in the frontier point evaluation function, which greatly improves the exploration efficiency.

B. Hybrid Mapping System

In order to provide as comprehensive information as possible for robot tasks, hybrid mapping systems have been extensively studied. In this section, the related work is classified according to the structures created for hybrid mapping. The first group pertains to works that generated 2D occupancy grid and topological map [13], [14]. In Zhang's work [14], the idea of Voronoi diagrams was utilized to construct a topological map after building a metric map. In [13], metric and topological maps were constructed in real time, and priority values were assigned to topological nodes according to their environment regions, so as to realize the graph exploration algorithm based on the priority of topological nodes.

The second group consists of a hybrid map composed of 3D point clouds and topological maps [18], [19]. In the work [18], a topological representation of free space maps to navigation graphs and convex voxel clusters was proposed. To improve the efficiency of global path planning, [19] built the topological map using both map points and trajectories of visual SLAM. The first two groups share a common problem: these hybrid maps cannot help the robot understand the environment like humans. If the target is obstructed by obstacles, the robot may not realize it even when it is close to the target. Adding semantic information to the region can avoid this problem. Following this, the third group aims to add semantic information to the hybrid map. The third group added semantic information to the hybrid metric and topological maps [16], [20], [21], [22], [23]. In [23], each node of the topological map contains a set of images from the region as semantic information, along with added metric information. In [16], the topological global representation and 3D dense submaps were maintained as a hybrid global map, which could be built by using a standard CPU, reducing the computational resources required. In [21], both unoccupied and occupied areas were characterized by voronoi diagrams, with recognized and classified objects from camera views placed in the topological nodes.

Although hybrid map systems have been studied extensively before, the types of maps that can be constructed simultaneously via mobile robots has not been comprehensive enough. Thus this work aims to fill this gap.

III. Method

A. Preliminaries: RRT-Based Exploration

RRT-based exploration [10] is a classical autonomous exploration method. An environment is classified as known space ($\boldsymbol{S}_{know}$) which has been explored and unknown space ($\boldsymbol{S}_{unkn}$) which has not been explored. $\boldsymbol{S}_{know}$ is classified as obstacle space ($\boldsymbol{S}_{obs}$) where the robot can not move due to the existing obstacles and unoccupied free space ($\boldsymbol{S}_{free}$). The goal of autonomous exploration is to explore $\boldsymbol{S}_{unkn}$. To this end, the model firstly generates random points ($\boldsymbol{P}_r$, as grey points in Fig. 3). Then, based on the robot's initial location ($\boldsymbol{L}_{init}$, as red points in Fig. 3) and $\boldsymbol{P}_r$, a tree structure originating from $\boldsymbol{L}_{init}$ is growing to cover $\boldsymbol{P}_r$. Frontier points

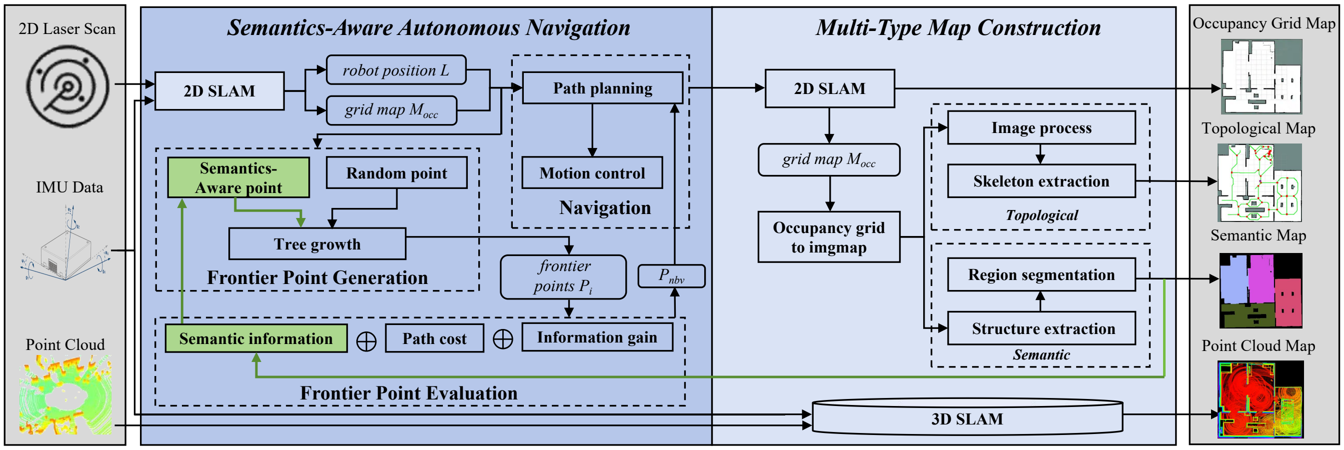

Fig. 2: The overview of our semantics-aware autonomous exploration model. The semantics-aware parts are shaded in green.

$\boldsymbol{P}_i$ (as green points in Fig. 3) are computed based on the tree branches and unknown space. Coarsely, $\boldsymbol{P}_i$ are points on the tree branches, and $\boldsymbol{P}_i$ are in $\boldsymbol{S}_{unkn}$, thus $\boldsymbol{P}_i$ are the guidance of the moving direction of the robot. Finally, the next-to-move point is selected from $\boldsymbol{P}_i$ according to the evaluation function to guide the autonomous exploration of the robot.

B. Overview

Taking 2D laser scan, IMU data, and point cloud data as input, the model outputs four kinds of maps through two key modules, namely the semantic-aware autonomous navigation module and multi-type map construction module. In the semantic-aware autonomous navigation module, frontier point generation mechanism outputs frontier points $\boldsymbol{P}_i$ based on the 2D occupancy grid map $\boldsymbol{M}_{occ}$ and the robot position $\boldsymbol{L}$. Frontier points $\boldsymbol{P}_i$ are then provided to the frontier point evaluation function, which outputs the robot's next best viewpoint goal $\boldsymbol{P}_{nbv}$. Path planning is conducted in $\boldsymbol{M}_{occ}$ based on $\boldsymbol{P}_{nbv}$ and $\boldsymbol{L}$, to guide the robot to move to $\boldsymbol{P}_{nbv}$. In the multi-type map construction module, four kinds of maps are constructed and updated.

C. Semantics-Aware Autonomous Navigation

Frontier points locate near to $\boldsymbol{S}_{unkn}$, thus they are important signals to guide the robot to explore $\boldsymbol{S}_{unkn}$. Since frontier point generation in RRT-based exploration relies on random sampling, the robot's exploration behavior easily result in excessively-repeated explorations for the same region. To address this issue, we propose a semantic-aware frontier point generation mechanism and semantic-aware frontier evaluation function.

1) Semantic-aware frontier point generation: As shown in Fig. 3, since the original frontier point generation mechanism does not consider regional semantics, the frontier point near to the bigger unknown space is easily selected as the next-to-move point, leading to that the robot needs to come back again to explore the smaller unknown space in the current region. In big and complex environments, excessively-repeated explorations occur frequently.

To alleviate the excessively-repeated explorations, we firstly introduce the semantic-aware point $\boldsymbol{P}_s$ (as yellow point in Fig. 3), which meet the condition that $\boldsymbol{P}_s$ are within the current semantic region, and $\boldsymbol{P}_s$ is on the frontier, and $\boldsymbol{P}_s$ is the closest to the robot. In conventional methods, the tree structure is growing based on random points $\boldsymbol{P}_r$. In our method, the tree structure is growing based on both $\boldsymbol{P}_r$ and $\boldsymbol{P}_s$. We propose a dynamic probability mechanism to select the sampling point (denoted as $\boldsymbol{P}_{sam}$), and $\boldsymbol{P}_{sam}$ further control the growing trend of tree structure, which is formulated as follow.

$$\begin{cases} p(\boldsymbol{P}_{sam} = \boldsymbol{P}_r) = \dfrac{1}{1 + k \cdot t} \\ p(\boldsymbol{P}_{sam} = \boldsymbol{P}_s) = \dfrac{k \cdot t}{1 + k \cdot t} \end{cases} \tag{1}$$

where $p(\boldsymbol{P}_{sam} = \boldsymbol{P}_r)$ denotes the probability that $\boldsymbol{P}_r$ is selected as $\boldsymbol{P}_{sam}$, $p(\boldsymbol{P}_{sam} = \boldsymbol{P}_s)$ denotes the probability that $\boldsymbol{P}_s$ is selected as $\boldsymbol{P}_{sam}$, t is a dynamic value signalling the exploration time in the current semantic region, and k is a fixed parameter. We can observe that, with the increasing of t, $p(\boldsymbol{P}_{sam} = \boldsymbol{P}_s)$ becomes larger, which encourages the tree to grow to the unknown space in the current semantic region (as yellow point in Fig. 3).

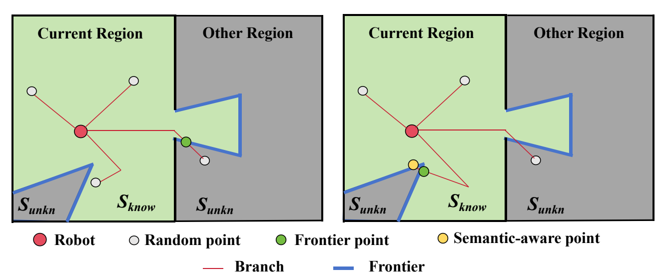

Fig. 3: Comparison of original frontier point generation (left) and semantic-aware frontier point generation (right).

The tree structure is determined based on $\boldsymbol{P}_{sam}$. Given the tree structure and unknown space $\boldsymbol{S}_{unkn}$, a set of frontier points $\boldsymbol{F}$ are generated by judging whether the tree structure crosses with $\boldsymbol{S}_{unkn}$:

$$\boldsymbol{F} = \{\boldsymbol{P}_i \mid i = 1, 2, ..., n\} \tag{2}$$

We note that the selection of $\boldsymbol{P}_s$ is based on semantic map, as the green feedback line in Fig. 2. The process of generating the semantic map will be detailed in the multi-type map construction section.

2) Semantic-aware frontier evaluation function: After obtaining a set of frontier points, conventional methods evaluate each frontier point to determine the best viewpoint goal $\boldsymbol{P}_{nbv}$, by considering the information gain $\boldsymbol{G}(\boldsymbol{P}_i)$ and path cost $\boldsymbol{C}(\boldsymbol{P}_i)$. Differently, we propose the semantic-aware frontier evaluation function that also takes the semantic region information into consideration.

$\boldsymbol{G}(\boldsymbol{P}_i)$ assesses the areas of unknown and known regions in a square surrounding frontier point $\boldsymbol{P}_i$, which is defined as follow.

$$\begin{aligned} \boldsymbol{G}(\boldsymbol{P}_i) &= f_s(g_{unkn}) - f_s(g_{know}), \\ g_{unkn} &\in \boldsymbol{S}_{unkn} \;,\; g_{know} \in \boldsymbol{S}_{know} \end{aligned} \tag{3}$$

where g_{unkn} denotes the unknown region in the square and g_{know} denotes the area of known region in the square, and $f_s()$ is the function to compute the areas of g_{unkn} and g_{know}. $\boldsymbol{C}(\boldsymbol{P}_i)$ evaluates the distance between $\boldsymbol{L}$ and $\boldsymbol{P}_i$:

$$\boldsymbol{C}(\boldsymbol{P}_i) = \|\boldsymbol{P}_i - \boldsymbol{L}\| \tag{4}$$

In our proposed semantic-aware frontier evaluation function, the semantic region information is also considered. If $\boldsymbol{P}_i$ and the robot are located in the same region (i.e., *flag*=1), a positive reward $\boldsymbol{A}(\boldsymbol{P}_i)$ is added to the evaluation function. Otherwise, a negative reward $\boldsymbol{A}(\boldsymbol{P}_i)$ is added to the evaluation function, which is formulated as follow.

$$S(\boldsymbol{P}_i) = \begin{cases} 3 \cdot \boldsymbol{G}(\boldsymbol{P}_i) - \boldsymbol{C}(\boldsymbol{P}_i) + \boldsymbol{A}(\boldsymbol{P}_i) \;,\; flag = 1 \\ 3 \cdot \boldsymbol{G}(\boldsymbol{P}_i) - \boldsymbol{C}(\boldsymbol{P}_i) - \boldsymbol{A}(\boldsymbol{P}_i) \;,\; flag = 0 \end{cases} \tag{5}$$

where $\boldsymbol{A}(\boldsymbol{P}_i)$ is set as an experimental value, $S(\boldsymbol{P}_i)$ denotes the score of $\boldsymbol{P}_i$. The frontier point with the highest score is selected as the next best viewpoint goal $\boldsymbol{P}_{nbv}$ to perform autonomous navigation. Our semantic-aware frontier evaluation function encourages the robot to fully explore the current region before moving to the other region.

D. Multi-Type Map Construction

When a mobile robot is performing autonomous navigation, multi-type maps are constructed at the same time. The main challenge of multi-type maps construction is aligning the coordinate of multi-type maps and coordinating the computation threads of multi-type map construction.

2D occupancy grid map $\boldsymbol{M}_{occ}$ is constructed by Cartographer SLAM [24] using laser scan and IMU data. To guarantee the coordinate consistency of maps, we construct other kinds of maps using the reference frame in $\boldsymbol{M}_{occ}$.

Topological map and semantic map generation are based on the occupancy grid map image, which is converted from $\boldsymbol{M}_{occ}$ using **Algorithm 1**. The first step is to create a matrix $\boldsymbol{M}_{img}$. Next, the grids in $\boldsymbol{M}_{occ}$ are traversed to judge whether they belong to $\boldsymbol{S}_{unkn}$, $\boldsymbol{S}_{free}$ or $\boldsymbol{S}_{obs}$. The corresponding pixels in $\boldsymbol{M}_{img}$ are then respectively set to grey, white, and black.

In topological map construction, to reduce measurement noise, we firstly apply binarization and morphological opening to filter out noise points. Then, the skeleton of topological map is extracted by thinning $\boldsymbol{M}_{img}$ [25] in a traversing manner with 3×3 matrix. The extracted skeleton elements are set to 1, and other elements are set to 0.

Algorithm 1: Occupancy grid to image map

Input: $\boldsymbol{M}_{occ}$
Output: $\boldsymbol{M}_{img}$

```
Create a matrix M_img ← height(M_occ), width(M_occ)
for i=1 to height(M_occ) do
    for j=1 to width(M_occ) do
        g(i,j) ← M_occ(i,j)
        if g(i,j) ∈ S_unkn then
            M_img(i,j) ← grey;
        end
        if g(i,j) ∈ S_free then
            M_img(i,j) ← white;
        end
        if g(i,j) ∈ S_obs then
            M_img(i,j) ← black;
        end
    end
end
```

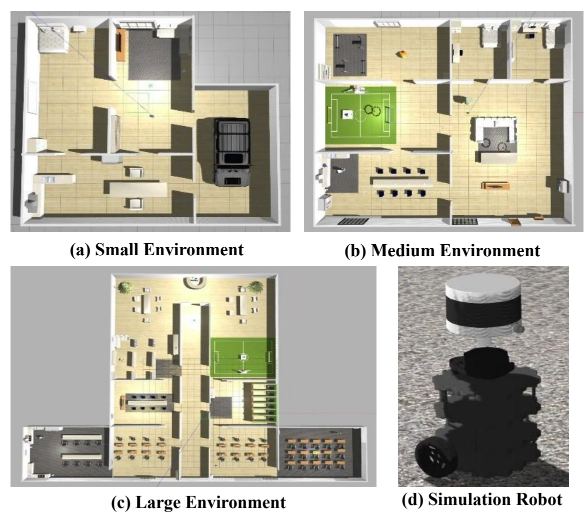

Fig. 4: Simulation environment and simulation robot.

In semantic map construction, referring to the processing of ROSE[2] [26], the construction procedure consists of the following steps. Firstly, structural features and wall lines of the environment are extracted from $\boldsymbol{M}_{img}$. Secondly, based on the structural features and wall lines, the geometric shapes of different regions are reconstructed. Finally, different regions are assigned with different semantic numbers and colors. The semantic region information is feed back to the module of semantic-aware autonomous navigation to support the generation of $\boldsymbol{P}_s$ and the evaluation of $\boldsymbol{P}_i$.

3D point cloud map is constructed using IMU data and point cloud data through LIO-SAM [27].

IV. Experiment

A. Settings

1) Simulation environments and robot: We set up three simulation environments using Gazebo [28], including a small house ($187m^2$), a medium house ($450m^2$), and a large

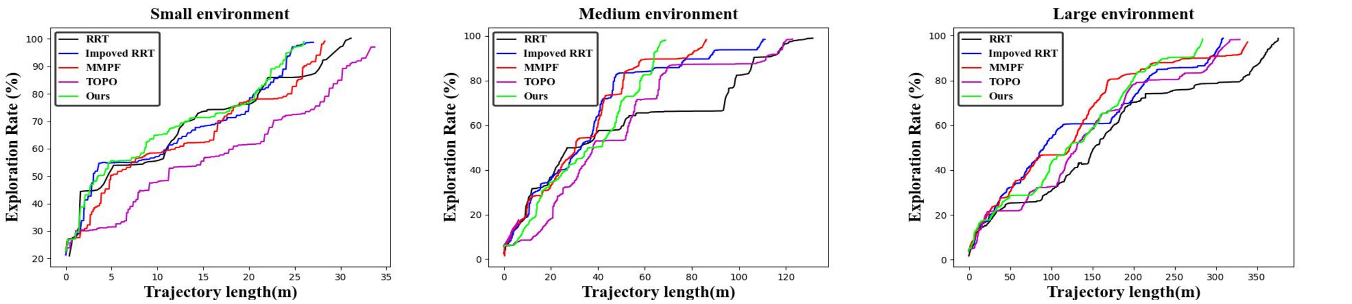

Fig. 5: Growing trend of exploration rate corresponding to the increasing exploration trajectory length.

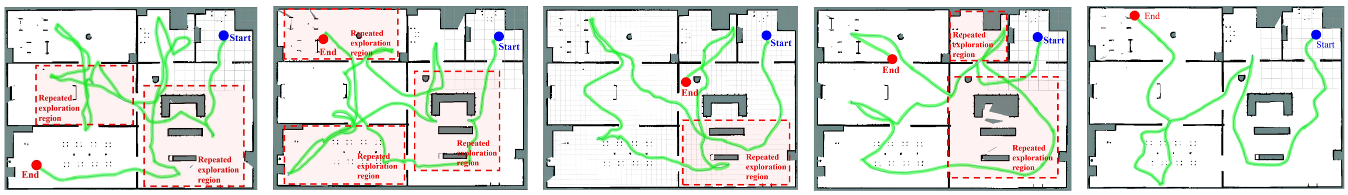

(a) RRT (b) Improved RRT (c) MMPF (d) TOPO (e) Our method

Fig. 6: Comparison of exploration trajectories. Red boxes indicate repeated exploration region.

office ($1160m^2$), as shown in Fig. 4. The Turtlebot3 Burger robot is used as the simulation robot, which is equipped with a 360^o laser scanner and a velodyne VLP-16 Lidar.

2) Metrics: The performance of an autonomous exploration model is evaluated by three metrics, including exploration time (i.e., the time consumption for exploring the whole environment), exploration trajectory length (i.e., the length of exploration trajectory for exploring the whole environment), and exploration rate (the ratio of the explored region to the whole environment).

3) Baselines: Four baseline methods, includes original RRT [10], TOPO [15], improved RRT and MMPF (proposed in [17]), are used in the experiments. RRT based methods are classical and commonly-used in autonomous exploration. MMPF [17], and TOPO [15] are recently-proposed methods with publicly-available codes.

TABLE I: Exploration time and trajectory length comparison. T: Exploration time (s), L: Trajectory length (m). The best result is in bold.

Methods	Small		Medium		Large	
	T	L	T	L	T	L
RRT [10]	171	31	593	131	1838	375
Improved RRT [17]	162	27	436	112	1282	306
MMPF [17]	125	28	350	87	1267	338
TOPO [15]	**118**	33	414	119	1054	329
Ours	126	**25**	**292**	**68**	**1018**	**283**

B. Autonomous Exploration Comparison and Analysis

1) Exploration rate and trajectory length analysis: Fig. 5 shows the growing trend of exploration rate corresponding to the increasing exploration trajectory length in small, medium, and large environments. We define that if exploration rate reaches 98%, an environment is supposed to be fully explored. We can observe from Fig. 5 that all models can fully explore the environment if exploration trajectory length is not limited. However, other models ask for longer exploration trajectory to achieve full environment exploration, especially in medium and large environments that are bigger and more complex. In addition, when other models are exploring the medium and large environment, there exist cases that exploration rate is not changing even though the length of the trajectory is increasing, implying that the robot is repeatedly moving in the previously-explored region. Instead, these cases are not frequently happened for our model.

2) Exploration time and trajectory length analysis: We conducted the experiments to compare the exploration time and trajectory length of our model and baselines, and results in small, medium, and large environments are reported in Tab. I. Our model asks for the least exploration time and the shortest exploration trajectory length in both medium and large environments. For example, compared with the second best result, our model achieves **16.6%** exploration time reduction and **21.8%** exploration trajectory length reduction in medium environment.

The superiority of our model is attributed to the proposed semantic-aware frontier point selection mechanism and frontier point evaluation function to avoid the excessively-repeated explorations for the same region. For further analysis, as shown in Fig. 6, we illustrated the exploration trajectories of different models in the medium environment. In the figure, the repeatly-explored regions are denoted by the red boxes. We can observe that other model make the robot enter and exit the same region more than one time to achieve the full exploration, while our model only asks for the robot to explore a region once, which significantly reduces the exploration time and trajectory length.

C. Muti-Type Map Construction Comparison and Analysis

Richer types of maps could support wider range of downstream tasks and applications. For example, the occupancy grid map and topological map are important for the path planning task [30], the point cloud map is essential for

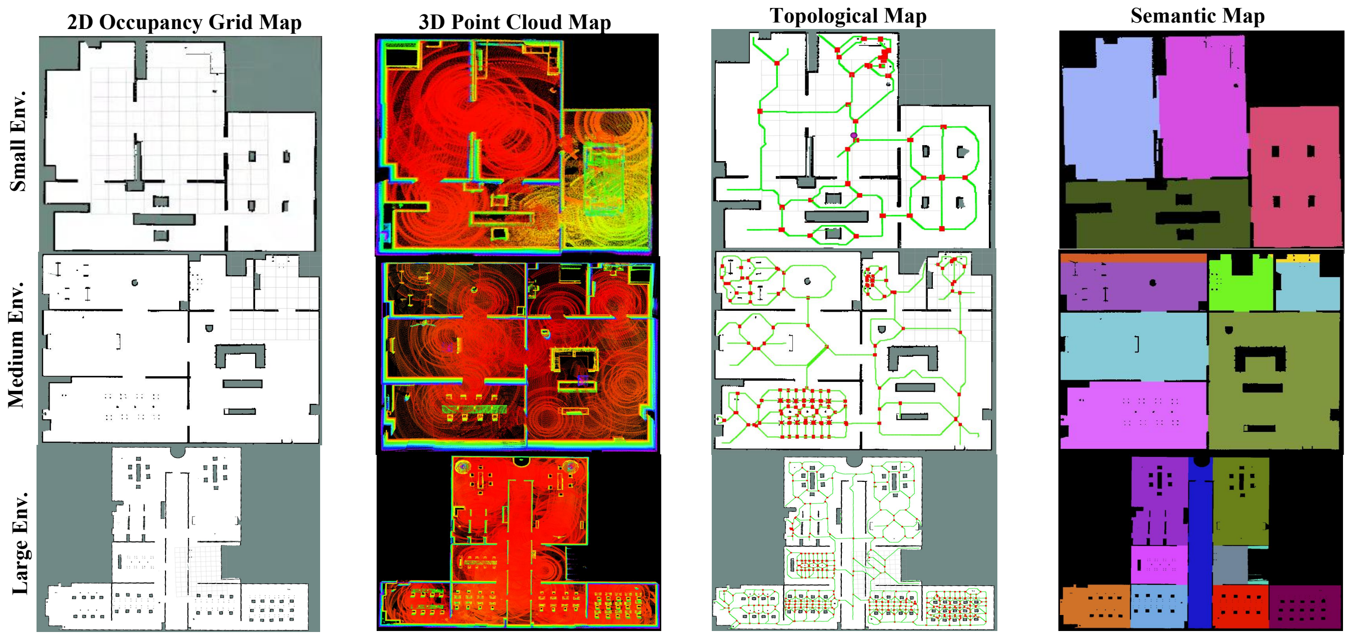

Fig. 7: Four kinds of maps constructed by our semantics-aware autonomous exploration model.

TABLE II: The types of maps constructed by previous models and our model. M1-M4 represents different types of maps. M1: 2D Occupancy grid map, M2: 3D Point cloud map, M3: Topological map, M4: Semantic map.

Methods	M1	M2	M3	M4
Blochliger et al. [18]ICRA'2018		✓	✓	
Gomez et al. [16]ICRA'2020		✓	✓	
Datta et al. [13]IROS'2021	✓		✓	
Wang et al. [6]RAL'2021	✓			✓
Liu et al. [20]IROS'2022		✓	✓	✓
Zhang et al. [15]RAL'2022	✓		✓	
Ishikawa et al. [29]SMC'2023	✓			✓
Ours	✓	✓	✓	✓

the robot localization and 3D detection [31] tasks, and the semantic map could support various human-robot-interaction applications that ask for semantic-level scene understanding. However, after reviewing the existing works in recent years, we find two or three kinds of maps are constructed, as summarized in Tab. II. As far as we know, our model is the first one to simultaneously construct four kinds of maps. Fig. 7 illustrates the muti-map construction results of our model in three environments. It is not challenging to simultaneously construct many types of maps. Why do previous works only construct two or three kinds of maps? With the increasing of map types, many factors (e.g., computation thread conflict, map coordinate alignment, map storage, and map updating frequency) need to be taken into consideration. Computation thread conflict and map coordinate alignment have been well handled in our method. In the following, we analyze the update time and storage size of maps.

Tab. III reports the detailed update time and storage size of each kind of map in three environments. Average update time for 2D occupancy grid map and topology map stays around $1s$ even in different simulation environments. The 3D point cloud map has the shortest update time, which fluctuates around $0.2s$ to quickly match the point cloud in consecutive frames. The semantic map requires longer update time ($2.2s$ to $3.1s$) in bigger environment. In practice, the exploration procedure is real-time under these update time conditions, the robot did not stop to wait the update of the certain map and the constructed maps are not deformed. For the map storage, we use different file formats to save the different types of maps: 2D occupancy grid map (PGM), 3D point cloud map (PCD), topological map (JPG), and semantic map (PNG). After the full exploration, the storage space of all maps is approximately 3.1MB for the small environment, 7.5MB for the medium environment, and 17.4MB for the large environment, respectively. Standard industrial computers can fulfill these storage needs.

TABLE III: Storage size and update time of multi-type maps. S : storage size (KB), U : update time (s).

Map types	Small		Medium		Large	
	S	U	S	U	S	U
2D Occupancy grid	509.7	0.9	707.0	0.9	798.7	1.0
3D Point cloud	2604.3	0.2	6867.3	0.2	16862.5	0.2
Topological	23.5	1.1	52.1	1.0	136.4	1.0
Semantic	6.1	2.2	8.6	2.6	18.3	3.1

V. Conclusion

In this paper, we propose a semantics-aware autonomous exploration model, which is able to avoid excessively-repeated explorations for the same region. The multi-type map construction method allows to simultaneously construct four kinds of maps in unknown indoor environments. Experimental results demonstrate that our system not only improves exploration efficiency but also provide multi-type map construction. In the future, we plan to extend our model to outdoor scenarios.

References

[1] B. Yamauchi, “A frontier-based approach for autonomous exploration,” in *Proceedings of the International Symposium on Computational Intelligence in Robotics and Automation (CIRA’97.’) Towards New Computational Principles for Robotics and Automation’*, 1997, pp. 146–151.

[2] A. Batinovic, T. Petrovic, A. Ivanovic, F. Petric, and S. Bogdan, “A multi-resolution frontier-based planner for autonomous 3d exploration,” *IEEE Robotics and Automation Letters (RA-L)*, vol. 6, no. 3, pp. 4528–4535, 2021.

[3] P. Zhong, B. Chen, S. Lu, X. Meng, and Y. Liang, “Information-driven fast marching autonomous exploration with aerial robots,” *IEEE Robotics and Automation Letters (RA-L)*, vol. 7, no. 2, pp. 810–817, 2021.

[4] C. Stachniss, G. Grisetti, and W. Burgard, “Information gain-based exploration using rao-blackwellized particle filters.” in *Robotics: Science and systems(RSS)*, 2005, pp. 65–72.

[5] A. Visser and B. Slamet, “Balancing the information gain against the movement cost for multi-robot frontier exploration,” in *Proceedings of the Second European Robotics Symposium (EUROS)*, 2008, pp. 43–52.

[6] C. Wang, D. Zhu, T. Li, M. Q.-H. Meng, and C. W. De Silva, “Efficient autonomous robotic exploration with semantic road map in indoor environments,” *IEEE Robotics and Automation Letters (RA-L)*, vol. 4, no. 3, pp. 2989–2996, 2019.

[7] T. Lai, F. Ramos, and G. Francis, “Balancing global exploration and local-connectivity exploitation with rapidly-exploring random disjointed-trees,” in *Proceedings of the International Conference on Robotics and Automation (ICRA)*, 2019, pp. 5537–5543.

[8] S. LaValle, “Rapidly-exploring random trees: A new tool for path planning,” Oct. 1998.

[9] A. Quattrini Li, “Exploration and mapping with groups of robots: Recent trends,” *Current Robotics Reports*, vol. 1, pp. 227–237, 2020.

[10] H. Umari and S. Mukhopadhyay, “Autonomous robotic exploration based on multiple rapidly-exploring randomized trees,” in *Proceedings of the IEEE/RSJ International Conference on Intelligent Robots and Systems (IROS)*, 2017, pp. 1396–1402.

[11] X. Tian, B. Li, Y. Du, and M. Wang, “Robot autonomous eploration and map building method,” in *Proceedings of the International Conference on Robotics and Automation in Industry (ICRAI)*, 2023, pp. 1–6.

[12] D. Jianhao, L. Meiqin, and S. Weihua, “Efficient exploration for real-time robot indoor 3d mapping,” in *Proceedings of the Chinese Control Conference (CCC)*, 2015, pp. 6078–6083.

[13] S. Datta and S. Akella, “Prioritized indoor exploration with a dynamic deadline,” in *Proceedings of the IEEE/RSJ International Conference on Intelligent Robots and Systems (IROS)*, 2021, pp. 3131–3137.

[14] Q. Zhang, *Autonomous indoor exploration and mapping using hybrid metric/topological maps, Ph.D. dissertation*, 2015.

[15] Z. Zhang, J. Yu, J. Tang, Y. Xu, and Y. Wang, “Mr-topomap: Multi-robot exploration based on topological map in communication restricted environment,” *IEEE Robotics and Automation Letters (RA-L)*, vol. 7, no. 4, pp. 10 794–10 801, 2022.

[16] C. Gomez, M. Fehr, A. Millane, A. C. Hernandez, J. Nieto, R. Barber, and R. Siegwart, “Hybrid topological and 3d dense mapping through autonomous exploration for large indoor environments,” in *Proceedings of the IEEE International Conference on Robotics and Automation (ICRA)*, 2020, pp. 9673–9679.

[17] J. Yu, J. Tong, Y. Xu, Z. Xu, H. Dong, T. Yang, and Y. Wang, “Smmr-explore: Submap-based multi-robot exploration system with multi-robot multi-target potential field exploration method,” in *Proceedings of the IEEE International Conference on Robotics and Automation (ICRA)*, 2021, pp. 8779–8785.

[18] F. Blochliger, M. Fehr, M. Dymczyk, T. Schneider, and R. Siegwart, “Topomap: Topological mapping and navigation based on visual slam maps,” in *Proceedings of the IEEE International Conference on Robotics and Automation (ICRA)*, 2018, pp. 3818–3825.

[19] W. Xue, R. Ying, Z. Gong, R. Miao, F. Wen, and P. Liu, “Slam based topological mapping and navigation,” in *Proceedings of the IEEE/ION Position, Location and Navigation Symposium (PLANS)*, 2020, pp. 1336–1341.

[20] H. Liu, H. Huang, S.-K. Yeung, and M. Liu, “360st-mapping: An online semantics-guided topological mapping module for omnidirectional visual slam,” in *Proceedings of the IEEE/RSJ International Conference on Intelligent Robots and Systems (IROS)*, 2022, pp. 802–807.

[21] A. Mora, C. Gomez, A. C. Hernandez, and R. Barber, “Topo-geometric mapping based on voronoi diagrams and bounding polygons,” in *Proceedings of the International Conference on Control, Automation and Robotics (ICCAR)*, 2022, pp. 105–110.

[22] R. C. Luo and W. Shih, “Autonomous mobile robot intrinsic navigation based on visual topological map,” in *Proceedings of the IEEE International Symposium on Industrial Electronics (ISIE)*, 2018, pp. 541–546.

[23] F. Üzer, H. Korrapati, E. Royer, Y. Mezouar, and S. Lee, “Vision-based hybrid map building for mobile robot navigation,” in *Proceedings of the Intelligent Autonomous Systems (IAS)*, 2016, pp. 135–146.

[24] W. Hess, D. Kohler, H. Rapp, and D. Andor, “Real-time loop closure in 2d lidar slam,” in *Proceedings of the IEEE International Conference on Robotics and Automation (ICRA)*, 2016, pp. 1271–1278.

[25] T. Y. Zhang and C. Y. Suen, “A fast parallel algorithm for thinning digital patterns,” *Communications of the ACM*, vol. 27, no. 3, pp. 236–239, 1984.

[26] M. Luperto, T. P. Kucner, A. Tassi, M. Magnusson, and F. Amigoni, “Robust structure identification and room segmentation of cluttered indoor environments from occupancy grid maps,” *IEEE Robotics and Automation Letters (RA-L)*, vol. 7, no. 3, pp. 7974–7981, 2022.

[27] T. Shan, B. Englot, D. Meyers, W. Wang, C. Ratti, and D. Rus, “Lio-sam: Tightly-coupled lidar inertial odometry via smoothing and mapping,” in *Proceedings of the IEEE/RSJ International Conference on Intelligent Robots and Systems (IROS)*, 2020, pp. 5135–5142.

[28] N. Koenig and A. Howard, “Design and use paradigms for gazebo, an open-source multi-robot simulator,” in *Proceedings of the IEEE/RSJ International Conference on Intelligent Robots and Systems (IROS)*, 2004, pp. 2149–2154.

[29] T. Ishikawa, A. Taniguchi, Y. Hagiwara, and T. Taniguchi, “Active semantic mapping for household robots: rapid indoor adaptation and reduced user burden,” in *Proceedings of the IEEE International Conference on Systems, Man, and Cybernetics (SMC)*, 2023, pp. 3116–3123.

[30] X. Wang, K. Tang, X. Dai, J. Xu, Q. Du, R. Ai, Y. Wang, and W. Gu, “S 4 tp: Social-suitable and safety-sensitive trajectory planning for autonomous vehicles,” *IEEE Transactions on Intelligent Vehicles (TIV)*, 2023.

[31] Y. Tian, X. Zhang, X. Wang, J. Xu, J. Wang, R. Ai, W. Gu, and W. Ding, “Acf-net: Asymmetric cascade fusion for 3d detection with lidar point clouds and images,” *IEEE Transactions on Intelligent Vehicles (TIV)*, pp. 1–12, 2023.